Published in final edited form as:
Dev Biol. 2011 July 1; 355(1): 43–54. doi:10.1016/j.ydbio.2011.04.019.

Disrupted dorsal neural tube BMP signaling in the cilia mutant *Arl13b*^{hnn} stems from abnormal Shh signaling

Vanessa L. Horner and **Tamara Caspary**[1]
Department of Human Genetics, Emory University School of Medicine, Atlanta, GA 30322, USA

Abstract

In the embryonic neural tube, multiple signaling pathways work in concert to create functional neuronal circuits in the adult spinal cord. In the ventral neural tube, Sonic hedgehog (Shh) acts as a graded morphogen to specify neurons necessary for movement. In the dorsal neural tube, bone morphogenetic protein (BMP) and Wnt signals cooperate to specify neurons involved in sensation. Several signaling pathways, including Shh, rely on primary cilia in vertebrates. In this study, we used a mouse mutant with abnormal cilia, *Arl13b*^{hnn}, to study the relationship between cilia, cell signaling, and neural tube patterning. *Alr13b*^{hnn} mutants have abnormal ventral neural tube patterning due to disrupted Shh signaling; in addition, dorsal patterning defects occur, but the cause of these is unknown. Here we show that the *Arl13b*^{hnn} dorsal patterning defects result from abnormal BMP signaling. In addition, we find that Wnt ligands are abnormally expressed in *Arl13b*^{hnn} mutants; surprisingly, however, downstream Wnt signaling is normal. We demonstrate that Arl13b is required non-autonomously for BMP signaling and Wnt ligand expression, indicating that the abnormal Shh signaling environment in *Arl13b*^{hnn} embryos indirectly causes dorsal defects.

Keywords

cilia; dorsal; neural tube; patterning; signaling; Arl13b

Introduction

Our ability to sense and respond to stimuli depends on neural activity in the spinal cord. Broadly speaking, cells in the dorsal half of the spinal cord integrate and relay information from sensory neurons in the periphery to the brain, whereas cells in the ventral half of the spinal cord transmit signals from the brain to muscles for movement. These cellular subtypes must be positioned correctly within the spinal cord for proper neuronal connections to be made. This critical spatial specification is established during embryonic development via signals sent to naïve cells in the neural tube.

The molecular natures of some of the early signals that specify neural cell identity have already been defined. In the ventral neural tube, Sonic hedgehog (Shh) becomes distributed as a gradient, with the highest concentration of Shh at the ventral-most position, the floor

[1]Corresponding author: 615 Michael Street, Suite 301, Whitehead Biomedical Research Building, Atlanta, GA 30322 Phone: 404-727-9862 Fax: 404-727-3949 tcaspar@emory.edu.

plate (FP). Shh signaling acts in a concentration- and time-dependent manner to specify five molecularly distinct classes of ventral neurons, including motor neurons (MN), and four types of ventral interneurons (V0-V3) (Supplemental Fig. 1A) [reviewed in (Ingham and McMahon, 2001;Jessell, 2000;Ribes and Briscoe, 2009)].

At the opposite pole of the neural tube, the roof plate (RP) emits signals that specify several of the dorsal-most interneurons (Lee, et al., 2000). Multiple members of the TGFβ signaling family are expressed in the RP, including *Bmp4*, *Bmp6*, *Bmp7*, and *Gdf7* [reviewed in (Liu and Niswander, 2005)]. Additionally, two members of the Wnt signaling family are expressed in the RP, *Wnt1* and *Wnt3a* (Parr, et al., 1993). Members of the TGFβ and Wnt families cooperate to establish dorsal progenitor domains 1–3 (Supplemental Fig. 1B). Mouse mutants with a complete loss of BMP signaling in the dorsal neural tube do not form the *Math1* progenitor domain, which in turn is required to specify the first class of dorsal interneurons (dI1s) (Bermingham, et al., 2001;Gowan, et al., 2001;Wine-Lee, et al., 2004). BMP signaling mutants also show reduced, but not abolished, *Wnt* expression, indicating that BMP signaling normally enhances *Wnt* expression (Wine-Lee, et al., 2004). Wnt signaling also promotes cell specification in the dorsal neural tube. Mice that are doubly mutant for *Wnt1* and *Wnt3a* show a reduction in the number of dI1-dI2s, which appears to stem from lowered *Math1* expression and loss of *Ngn1* expression (Muroyama, et al., 2002). Wnt signaling may act primarily through the bHLH transcription factor Olig3 to specify dorsal neurons, since Olig3 is essential to maintain proper expression of *Math1*, *Ngn1*, and *Ngn2* (Muller, et al., 2005). Canonical Wnt signaling through β-catenin is sufficient for *Olig3* expression, and mutation of *Olig3* reduces the number of dI1s and abolishes dI2-dI3s (Muller, et al., 2005;Zechner, et al., 2007).

Interactions among the Shh, BMP, and Wnt signaling pathways are necessary to establish proper patterning of the embryonic neural tube. BMP signaling must be actively repressed in the ventral neural tube; mice that are mutant for the notochord-derived BMP antagonist, *noggin*, lack FP cells and motor neurons in the ventral neural tube (McMahon, et al., 1998). Conversely, Shh signaling must be repressed in the dorsal neural tube. Inappropriately active Shh signaling in the dorsal neural tube can repress BMP ligand expression, thereby disrupting BMP signaling and dorsal patterning (Cho, et al., 2008). In chick, *Wnt1* and *Wnt3a* directly control the expression of *Gli3*, the main repressor of Shh signaling in the dorsal neural tube (Alvarez-Medina, et al., 2008). Finally, Gli3 repressor physically interacts with the downstream effectors of both BMP and Wnt signaling, the Smad proteins and β-catenin, respectively (Liu, et al., 1998;Ulloa, et al., 2007). Although these examples illustrate intimate connections between neural tube signaling pathways, the precise mechanisms underlying their interactions are just beginning to be investigated and understood.

In vertebrates, several signaling pathways require primary nonmotile cilia for cellular transduction, including Shh (Huangfu, et al., 2003), planar cell polarity (PCP) (Jones, et al., 2008;Ross, et al., 2005), and platelet-derived growth factor receptor α (PDGFRα) (Schneider, et al., 2005) [reviewed in (Veland, et al., 2009)]. Mouse embryos lacking the cilia protein Arl13b show left-right axis defects, polydactyly, and ventral neural tube patterning defects, all of which rely on Shh signaling (Caspary, et al., 2007;Garcia-Garcia, et al., 2005). Arl13b is a small GTPase of the Ras superfamily (Caspary, et al., 2007). A few members of this family are known to function in vesicle trafficking and microtubule dynamics, although the functions of most members of this family remain unknown (Antoshechkin and Han, 2002;Hoyt, et al., 1990;Kahn, et al., 2006;Li, et al., 2004;Radcliffe, et al., 2000;Zhou, et al., 2006). Within the cell, Arl13b localizes predominantly to cilia (Caspary, et al., 2007) and is absent in *Arl13b*^{hnn} mutants. An examination of cilia in *Arl13b*^{hnn} mutants revealed a defect in the ultrastructure of the axoneme, resulting in cilia

that are half the length of wild-type (Caspary, et al., 2007). *Arl13b*^{hnn} mutants have ventral neural tube patterning defects as a result of disrupted Shh signaling (Caspary, et al., 2007).

In addition to the ventral neural tube phenotypes described above, the *Arl13b*^{hnn} mutation also disrupts dorsal neural tube patterning: *Wnt1*, *Math1*, and *Mash1* are discontinuously expressed in the caudal neural tube (Caspary, et al., 2007). This observation is surprising, since Shh signaling is presumably repressed in the *Arl13b*^{hnn} dorsal neural tube by the normal Gli3 repressor activity (Caspary, et al., 2007). The dorsal phenotypes therefore raise the possibility that the signaling pathways involved in dorsal cell specification are disrupted in *Arl13b*^{hnn} mutants. Here we show that the *Arl13b*^{hnn} mutation disrupts the expression of BMP and Wnt ligands. Further, we demonstrate that BMP signaling is abnormal in the *Arl13b*^{hnn} dorsal neural tube, but canonical Wnt signaling is surprisingly unaffected. Since Gli3 has activity in *Arl13b*^{hnn} and has been tied to the Shh, BMP, and Wnt pathways, we use conditional experiments to test whether the dorsal role of Arl13b in regulating Gli3 is dependent on, or independent of, the ventral role of Arl13b in ventral patterning. Through this analysis we demonstrate that all patterning defects we observe in *Arl13b*^{hnn} mutants primarily result from the misregulation of Shh signaling in the ventral neural tube.

Materials and methods

Mouse strains

The *Arl13b*^{hnn} allele was generated by ENU mutagenesis and is a protein-null allele containing a splice site mutation that results in the excision of exon 2 (Caspary, et al., 2007). The conditional *Arl13b*^{LoxP} allele was generated via homologous recombination and mimics the splice site mutation of the original *hnn* allele by flanking exon 2 with *loxP* sites (Su, et al., in preparation). In BATgal transgenic mice, 7 TCF sites are fused to the *lacZ* gene to allow *in vivo* observation of canonical Wnt signaling via analysis of β-galactosidase activity (Maretto, et al., 2003). In *Pax3*$^{tm1\ (cre)Joe}$ transgenic mice (hereafter referred to as *Pax3-cre*), the endogenous *Pax3* promoter drives expression of Cre recombinase (Engleka, et al., 2005). In *Gt(ROSA)26Sor*^{tm1Sor} transgenic mice (hereafter referred to as ROSA26), *loxP* sites flank a STOP sequence upstream of the *lacZ* gene to monitor Cre-mediated recombination via analysis of β-galactosidase activity (Soriano, 1999). To facilitate the conditional removal of Arl13b in the dorsal neural tube, half the amount of endogenous Arl13b was removed by crossing one copy of the null *Arl13b*^{hnn} allele into the *Pax3-cre* background.

In situ hybridization

In situ hybridizations on frozen transverse sections and whole-mounted embryos were performed as described (Belo, et al., 1997;Schaeren-Wiemers and Gerfin-Moser, 1993). For each experiment at least 3 embryos of the same genotype and developmental stage were analyzed. Digoxigenin-labeled anti-sense RNA probes were synthesized from linearized plasmid DNA using RNA polymerase T3, T7, or Sp6 according to the manufacturer's instructions. *In situ* hybridization probes were as follows: *Msx1* (J. Corbin, Children's National Medical Center, Washington D.C.), *Lhx2* (E. Grove, University of Chicago, Chicago, IL), *Wnt1* and *Wnt3a* (A. McMahon, Harvard University, Boston MA), *Gdf7* (T. Jessel, Columbia University, New York, NY), *Math1* and *Mash1* (J. Johnson, UT Southwestern, Dallas, TX), *Axin2* (F. Costantini, Columbia University, New York, NY), *Gli1* and *Gli2* (A. Joyner, Sloan Kettering Institute, New York, NY), and *Gli3* (J. Eggenschwiler, Princeton University, Princeton, NJ).

Immunohistochemistry

Embryos were dissected and fixed for 1 hour in 4% paraformaldehyde (PFA) on ice. After fixation, embryos were immediately washed 4 times for 30 min in cold phosphate-buffered

saline (PBS) and incubated in 30% sucrose at 4°C overnight. Embryos were washed in Optimal Cutting Temperature (OCT) Compound 3 times for 15 min before embedding in OCT. We obtained 10-12-micron sections on a Leica CM1850 cryostat. Immunostaining was performed as described (Yamada, et al., 1993). Briefly, slides were washed 3 times for 5 min in PBS, and then blocked for 1 h at room temperature in PBS containing 10% heat-inactivated sheep serum and 0.1% triton-X. Slides were incubated with the following antibodies overnight at 4°C: rabbit polyclonal anti-Arl13b, 1:1500 (Caspary, et al., 2007), mouse monoclonal anti-Cre, 1:500 (Sigma), mouse polyclonal anti-HB9, 1:10 (Developmental Studies Hybridoma Bank), rabbit polyclonal anti-Olig2, 1:300 (Chemicon), rabbit polyclonal anti-Olig3, 1:5000, guinea pig anti-Tlx3, 1:10,000, and guinea pig anti-Foxd3, 1:5,000 (gifts from C. Birchmeier, Max Delbruck-Center for Molecular Medicine, Berlin, Germany), mouse monoclonal anti-BrdU, 1:100 (Sigma), and rabbit polyclonal phospho-histone H3, 1:1000 (Millipore). Primary antibody-bound slides were incubated for 1–2 h at room temperature with 1:200 Alexa Fluor 488- and 568-conjugated goat anti-mouse and goat anti-rabbit antibodies (Molecular Probes) and 1:6000 Hoechst 33342 (Molecular Probes). Slides were mounted in 80% glycerol and viewed within 24 h.

Bromodeoxyuridine (BrdU)

BrdU was injected intraperitoneally into pregnant females on embryonic day 10.5, at a final concentration of 50 μg/g body weight. Thirty min after injection, females were sacrificed and embryos were fixed for antibody staining as described above. Prior to the blocking step of antibody staining, sections were treated for antigen retrieval by covering slides with 10 mM sodium citrate and then steaming the slides for 15 min in an Oster steamer.

Staining for β-galactosidase activity

Staining for β-galactosidase activity was performed as described in (Nagy, et al., 2003). Briefly, embryos were fixed in 1M Phosphate Buffer containing 0.2% glutaraldehyde for 15–30 min at room temperature, and then washed in detergent rinse (Nagy, et al., 2003) 3 times for 15–30 min each. To observe β-galactosidase activity, embryos were incubated with staining solution (Nagy, et al., 2003) containing 0.1 mg/mL X-gal overnight at room temperature. To section X-gal-stained embryos, embryos were washed 2 times for 5 min in PBS, fixed in 4% PFA for 2 h at room temperature or overnight at 4°C, re-washed in PBS for 5 min, incubated in 30% sucrose overnight, and embedded in OCT as above. Slides containing 25-50-μM sections were washed 3 times for 5 min in PBS and mounted in 80% glycerol prior to viewing.

Microscopy

Images of whole embryos and neural tube sections were collected with a Leica MZFLIII stereomicroscope and a Leica DM6000 B upright fluorescence microscope, respectively. Q-capture and Simple PCI software were used to collect images. Adobe Photoshop CS2 was used to crop and adjust color, brightness, and contrast of images.

Cell counting and statistics

Cells in the neural tube were counted using Simple PCI software. A total of 15 neural tube sections from 3 *Arl13b*^{hnn} embryos were counted, and a total of 12 neural tube sections from 3 WT embryos were counted. The number of cells stained with BrdU (S phase) and the number of cells stained with phosphohistone H3 (M phase) were normalized to the total number of cells in the neural tube (stained with Hoechst). Statistical differences between WT and *Arl13b*^{hnn} were determined with a 2-tailed Student's t-test.

Results and discussion

Wnt ligands are abnormally expressed in the Arl13b^{hnn} neural tube, but downstream canonical Wnt signaling is normal

Two Wnt ligands are expressed in the neural tube roof plate, *Wnt1* and *Wnt3a*, and their combined loss results in lowered *Math1* expression and loss of *Ngn1* expression (Muroyama, et al., 2002;Parr, et al., 1993). *Wnt1* is aberrantly expressed in the *Arl13b^{hnn}* neural tube; caudal to the forelimb, *Wnt1* is expressed in discontinuous patches, with a region near the hindlimb showing complete loss of expression (Caspary, et al., 2007). We found that *Wnt3a* is also discontinuously expressed and absent in the *Arl13b^{hnn}* caudal neural tube (Fig. 1A, B). Since both *Wnt* ligands are lost in the same region, we next explored whether canonical Wnt signaling is disrupted in *Arl13b^{hnn}* mutant embryos. Canonical Wnt signaling can be visualized with tools that detect TCF/LEF transcription factor activity, the mediators of canonical Wnt signaling. In BATgal transgenic mice (Maretto, et al., 2003), seven TCF sites are fused to the lacZ gene to allow *in vivo* observation of canonical Wnt signaling via analysis of β-galactosidase activity. To analyze canonical Wnt signaling in *Arl13b^{hnn}* mutants, we obtained E9.5, E10.5, and E11.5 wild-type (WT) and *Arl13b^{hnn}* embryos carrying the BATgal transgene and stained them with *X-gal*. Canonical Wnt signaling was present at similar levels, places, and times in all WT and *Arl13b^{hnn}* mutants examined, in both whole embryos and neural tube sections at the hindlimb level (Fig. 2). In the WT caudal neural tube, canonical Wnt signaling is observed throughout most of the dorsal-ventral axis of the neural tube at E9.5 (Yu, et al., 2008), but by E10.5 and E11.5, canonical Wnt signaling is largely restricted to the dorsal-most third of the neural tube (Fig 2). In *Arl13b^{hnn}* mutants, Wnt signaling is likewise observed throughout the neural tube at E9.5 and limited to the dorsal neural tube at E10.5 and E11.5 (Fig. 2).

Another global measure of canonical Wnt signaling is expression of *Axin2*, a direct transcriptional target of canonical Wnt signaling (Jho, et al., 2002). The expression of *Axin2* in whole embryos and neural tube sections is indistinguishable between WT and *Arl13b^{hnn}* mutants (Fig. 1C, D). Moreover, canonical Wnt signaling controls the expression of *Olig3*, and we see that Olig3 protein is present at the correct time and place in the *Arl13b^{hnn}* dorsal neural tube (Fig. 1E-H). Since Olig3 is required to specify dI2 and dI3 interneurons (Muller, et al., 2005;Zechner, et al., 2007), we next examined whether these neurons are present in the *Arl13b^{hnn}* neural tube using homeodomain transcription factors that are differentially expressed in postmitotic neurons (Helms and Johnson, 2003;Qian, et al., 2002). We found that Foxd3^{+} (dI2) and Tlx3^{+} (dI3 and dI5) cells are specified in the *Arl13b^{hnn}* neural tube, although their patterning within the neural tube is not as precisely ordered as in WT (Fig 1E-H). For instance, the separation between dI3 and dI5 neurons is sharply distinct in WT, but appear to be more of a continuum in *Arl13b^{hnn}* (Fig. 1H).

In addition to cell fate, Wnt signaling controls cell proliferation in the neural tube (Cayuso and Marti, 2005;Dickinson, et al., 1994;Megason and McMahon, 2002). *Arl13b^{hnn}* mutants do not show gross errors in cell proliferation (Caspary, et al., 2007). However, to detect any subtle changes in cell proliferation, we quantified the number of proliferating cells in WT and *Arl13b^{hnn}* neural tubes by staining for BrdU, which marks S phase, and phospho-histone H3, which marks M phase, and normalized to the total number of cells in the neural tube (Fig. 3). We did not observe any difference in the number of cells in S phase ($p = 0.29$) or M phase ($p = 0.08$) in WT and *Arl13b^{hnn}* neural tubes (Fig. 3C). Taken together, these results indicate that, despite abnormal ligand expression, canonical Wnt signaling is unaffected in *Arl13b^{hnn}* mutants.

BMP signaling is aberrant in the Arl13b^{hnn} dorsal neural tube

Since Wnt ligand expression is disrupted in the *Arl13b*^{hnn} roof plate, we next explored whether TGFβ ligand expression is similarly disrupted. Several TGFβ ligands are expressed in the roof plate, including *Bmp4*, *Bmp6*, *Bmp7*, and *Gdf7*. The role of individual TGFβ ligands in dorsal neural tube patterning has remained elusive, due to functional redundancy or early embryonic lethality (Beppu, et al., 2000;Dudley, et al., 1995;Dudley and Robertson, 1997;Luo, et al., 1995;Lyons, et al., 1995;Mishina, et al., 1995;Winnier, et al., 1995;Zhang and Bradley, 1996). The exception is loss of *Gdf7*, which results in loss of dI1a neurons (Lee, et al., 1998). Since loss of *Gdf7* alone is sufficient to cause dorsal neural tube patterning defects, we used *in situ* hybridization to examine its expression in WT and *Arl13b*^{hnn} mutant embryos. We observed specific and strong staining in the WT neural tube along the entire rostral-caudal axis (Fig. 4A, C). Similar to the Wnt ligands, expression of *Gdf7* is largely absent and discontinuous in the caudal neural tube of *Arl13b*^{hnn} mutant embryos (Fig. 4B, D).

To see whether the abnormal *Gdf7* expression has downstream effects in *Arl13b*^{hnn} mutants, we next examined several BMP targets. An established read-out of BMP signaling is transcription of *Msx-1*, a homeobox transcription factor that acts as an effector of BMP signaling and whose expression is directly upregulated in response to BMP signaling (Furuta, et al., 1997;Liem, et al., 1997;Liu, et al., 2004). We observe similar levels of *Msx-1* in the limb buds and pharyngeal arches of WT and *Arl13b*^{hnn} mutant embryos, but *Msx-1* expression is discontinuous and largely absent in the caudal neural tube of *Arl13b*^{hnn} mutant embryos (Fig. 4E-H). Furthermore, BMP signaling is required for the specification of dI1 interneurons, and we found that expression of *Lhx2*, which marks dI1s, is discontinuous in the caudal neural tube (Fig. 4I-L). Together with the previous observations that *Math1*, *Wnt1*, and *Wnt3a* expression are disrupted, these results indicate that BMP signaling is aberrant in the dorsal neural tube of *Arl13b*^{hnn} mutants. These results are consistent with other mutants in which BMP signaling is lost, since total elimination of BMP receptors in the roof plate results in the loss of *Math1* and dI1s (Wine-Lee, et al., 2004). Furthermore, the discontinuous expression of *Wnt1* and *Wnt3a* in the *Arl13b*^{hnn} roof plate may stem from the disruption in BMP signaling, since BMP signaling mutants show reduced expression of Wnt ligands (Wine-Lee, et al., 2004).

Arl13b is required non-autonomously for BMP signaling and Wnt ligand expression

Since interactions between the Shh signaling pathway and dorsal signaling pathways are necessary to establish proper patterning of the neural tube, it is possible that the disruption of Shh signaling in the *Arl13b*^{hnn} neural tube indirectly disrupts BMP signaling and thus dorsal patterning. Alternatively, Arl13b might be directly required in the dorsal neural tube for BMP signaling and Wnt ligand expression. To distinguish these two possibilities, we used our conditional *Arl13b* allele, *Arl13b*^{LoxP}, in which *LoxP* sites flank the second exon of *Arl13b*, so that upon Cre-mediated recombination exon 2 is excised, resulting in a mutation that mimics the null *hnn* mutation (Su, et al., in preparation). We removed *Arl13b* exclusively in the dorsal neural tube by crossing *Arl13b*^{LoxP} mice to mice that express Cre recombinase under the control of the *Pax3* promoter (Engleka, et al., 2005). *Pax3* is expressed starting from E8.5, just as neurogenesis begins (Solloway and Robertson, 1999), and becomes restricted to the dorsal-most third of the dorsal neural tube. This cross also generated the appropriate control embryos that carry the *Arl13b*^{LoxP} conditional allele alone, or the *Pax3-cre* transgene alone.

Pax3-cre-mediated recombination occurs by E9.5, and Arl13b protein is removed in the dorsal neural tube beginning at E9.5—To monitor the spatial and temporal activity of *Pax3-cre*, we used the ROSA26 reporter, in which a STOP sequence

flanked by *loxP* sites is upstream of the *lacZ* gene (Soriano, 1999). Upon Cre-mediated recombination, β-galactosidase is expressed and can be visualized with *X-gal* staining. Thus, the ROSA26 reporter shows not only when and where Cre recombinase is expressed, but also the length of time necessary for recombination to occur. We crossed mice carrying *Pax3-cre* to the ROSA26 reporter line and dissected embryos at E8.5, E9.5, and E10.5. We did not detect recombination at E8.5, but at E9.5 and E10.5 β-galactosidase activity was observed in the neural tube, midbrain, hindbrain, somites, pharyngeal arches, and frontonasal prominence (Supplemental Fig. 2). Neural tube sections taken at the forelimb and hindlimb levels of *X-gal*-stained embryos show that recombination occurs only in the dorsal neural tube (Supplemental Fig. 2).

To detect when Arl13b protein is removed from the dorsal neural tube, we crossed mice carrying our $Arl13b^{LoxP}$ conditional allele to mice carrying *Pax3-cre* and dissected embryos at E9.5, E10.5, and E11.5. Neural tube sections of $Arl13b^{\Delta Pax3\text{-}cre}$ and control embryos were stained with antibodies against Arl13b and Cre. At E9.5 Cre recombinase is restricted to cells in or around the roof plate (Fig 5B). Arl13b protein can be visualized in the ventricular zone along most of the dorsal-ventral axis of the neural tube; however, where Cre is expressed, loss of Arl13b is already apparent (Fig. 5B). In E10.5 and E11.5 neural tube sections at the hindlimb level, Arl13b is absent where Cre is expressed, in the dorsal-most one third to one half of the neural tube (Fig. 5C-F). In summary, *Pax3-cre* drives expression of Cre recombinase at E8.5, recombination occurs in the neural tube by E9.5, and Arl13b protein is lost in the dorsal neural tube by E9.5-E10.5.

Based on these data and previous studies, we can make predictions regarding the embryonic stage at which we would expect to see a phenotype in our conditional mutants. To demonstrate that the roof plate is a source of signaling molecules necessary for dorsal interneuron specification, (Lee, et al., 2000) conditionally ablated the roof plate by driving the expression of diphtheria toxin in the roof plate via the *Gdf7* promoter. *Gdf7* is expressed at E9.5-E10.0 (Lee, et al., 2000). Prior to *Gdf7* expression and roof plate formation, *Msx1*, *Wnt1*, and *Wnt3a* are expressed in dorsal midline cells, presumably due to BMP signaling from the epidermal ectoderm. When the roof plate was removed at E9.5-E10.0, expression of *Msx1*, *Wnt1*, and *Wnt3a* was lost by E11.0. In another study, BMP receptors were removed in the neural tube at E9.5-E10.0 to completely eliminate BMP signaling (Wine-Lee, et al., 2004). In these mutants, *Math1* was expressed at E10.0, but lost by E10.5. These studies demonstrate that BMP signaling is required to maintain expression of dorsal patterning genes. Since the expression of genes that rely on BMP signaling was disrupted about 0.5-1 day after BMP signaling was removed in the above studies, we would expect to see any dorsal phenotypes in $Arl13b^{\Delta Pax3\text{-}cre}$ embryos between E10.5-E12.5.

Removing Arl13b exclusively in the dorsal neural tube permits proper Shh signaling in the ventral neural tube—The ability to distinguish whether loss of Arl13b directly or indirectly disrupts dorsal neural tube patterning depends on our prediction that selectively removing Arl13b in the dorsal neural tube will permit proper Shh signaling in the ventral neural tube. To ensure that ventral patterning is normal in $Arl13b^{\Delta Pax3\text{-}cre}$ embryos, we dissected $Arl13b^{\Delta Pax3\text{-}cre}$ embryos at E10.5 and E11.5 and stained neural tube sections with antibodies against HB9 and Olig2, which mark motor neurons (MNs) and progenitors of motor neurons (pMNs), respectively (Arber, et al., 1999;Novitch, et al., 2001). In $Arl13b^{hnn}$ mutant embryos, MNs and pMNs are dramatically expanded from their restricted domains in the ventral neural tube both ventrally and dorsally (Fig. 5G) (Caspary, et al., 2007). When Arl13b is removed only in the dorsal neural tube, however, we see that the domains of MNs and pMNs are identical to WT, confirming that Shh signaling and ventral patterning is normal in $Arl13b^{\Delta Pax3\text{-}cre}$ embryos (Fig. 5H-K).

Conditional loss of Arl13b results in postnatal death at P0—*Arl13b*^{hnn} embryos have several morphological defects, including exencephaly and spina bifida, and they die between E13.5-E14.5 (Caspary, et al., 2007). To determine whether *Arl13b*$^{\Delta Pax3\text{-}cre}$ embryos are viable, we performed timed matings and examined embryos at specific stages, as well as just after birth. We found *Arl13b*$^{\Delta Pax3\text{-}cre}$ embryos have no overt morphological defects and are indistinguishable from WT during embryogenesis (Table 1). However, at birth most *Arl13b*$^{\Delta Pax3\text{-}cre}$ pups died after an episode of observable gasping. We examined the internal organs of 2 of the *Arl13b*$^{\Delta Pax3\text{-}cre}$ mutants just after death and found that the stomachs contained air bubbles, consistent with a breathing problem. We did see one *Arl13b*$^{\Delta Pax3\text{-}cre}$ pup survive, indicating that escapers can occur; however, this mouse was severely runted and died by postnatal day 21. Therefore, *Arl13b*$^{\Delta Pax3\text{-}cre}$ mutants die shortly after birth at P0, likely due to a breathing problem.

Arl13b is not directly required in the dorsal neural tube for BMP signaling or Wnt ligand expression—If the observed *Arl13b*^{hnn} dorsal patterning defects are indirectly caused by disrupted Shh signaling, then removing Arl13b exclusively in the dorsal neural tube will allow normal dorsal signaling and patterning in the conditional *Arl13b*$^{\Delta Pax3\text{-}cre}$ mutants. Alternatively, if Arl13b is directly required in the dorsal neural tube, then loss of Arl13b in the dorsal neural tube will result in the dorsal signaling and patterning defects observed in *Arl13b*^{hnn} mutants (Figs. 1 and 4). We monitored BMP signaling via expression of *Msx1*, *Math1*, *Gdf7*, and *Lhx2*, as described above. In addition, we examined dorsal patterning via expression of *Wnt1*, *Wnt3a*, and *Mash1*.

The expression patterns of *Msx1* and *Math1* were examined in whole *Arl13b*$^{\Delta Pax3\text{-}cre}$ mutant embryos and their sibling controls from E10.5-E13.5. Unlike *Arl13b*^{hnn} mutants, where expression of these markers is discontinuous in the caudal neural tube, both *Msx1* and *Math1* are expressed continuously and at similar levels in the caudal neural tube of *Arl13b*$^{\Delta Pax3\text{-}cre}$ mutant embryos and their littermate controls at all stages examined (Fig. 6). There was some variation between experiments in the posterior boundary of expression (number of somites from the tip of the tail), but there was no consistent correlation between genotype and the posterior limit of expression. In addition, neural tube sections of E11.5 and E12.5 embryos taken at the hindlimb level show that the pattern of *Msx1* and *Math1* expression along the dorsal-ventral axis of the neural tube is similar in *Arl13b*$^{\Delta Pax3\text{-}cre}$ mutant and control embryos (Fig. 6). Since Lhx2 marks differentiated dI1s, we examined embryos at slightly later stages, E12.5-E14.5. In all embryos and at all stages examined, we detected no difference in the level of staining or pattern of *Lhx2* expression between *Arl13b*$^{\Delta Pax3\text{-}cre}$ mutant and control embryos (Fig. 7).

Since we interpreted the abnormal *Msx1*, *Math1*, and *Lhx2* expression in *Arl13b*^{hnn} embryos to result from the lack of *Gdf7* ligand, their presence in the conditional mutants predicts that *Gdf7* expression should be normal. Indeed, *Gdf7* is expressed continuously and at similar levels in all *Arl13b*$^{\Delta Pax3\text{-}cre}$ mutant and control embryos examined (Fig 8A-D). Finally, we examined *Wnt1*, *Wnt3a*, and *Mash1* expression at E11.5 and E12.5 in *Arl13b*$^{\Delta Pax3\text{-}cre}$ mutant and control embryos. Despite the abnormal expression of these genes in the *Arl13b*^{hnn} dorsal neural tube, we detected no differences in the level or expression pattern of any of these genes between *Arl13b*$^{\Delta Pax3\text{-}cre}$ mutant and control embryos (Fig. 8E-P).

Taken together, these data demonstrate that cells in the dorsal neural tube do not require Arl13b for TGFβ signaling or Wnt ligand expression, and the *Arl13b*^{hnn} dorsal neural tube defects are non-autonomous. Therefore, the dorsal patterning defects observed in *Arl13b*^{hnn} embryos are an indirect consequence of the abnormal Shh signaling environment in these embryos.

Subtle changes in Gli activator/Gli repressor ratios could influence BMP signaling

Shh signaling is mediated at the transcriptional level by three proteins in vertebrates: Gli1, Gli2, and Gli3 (Matise and Joyner, 1999). Gli1 behaves only as a transcriptional activator, while Gli2 and Gli3 can act as both transcriptional activators and repressors (Aza-Blanc, et al., 2000;Jacob and Briscoe, 2003). The graded response of cells in the ventral neural tube to Shh is mediated by the ratio of Gli activator (GliA) to Gli repressor (GliR) activity [reviewed in (Ribes and Briscoe, 2009)]. In mouse mutants that completely lack cilia, there is a loss of both GliA and GliR activity in the neural tube (Huangfu and Anderson, 2005;Liu, et al., 2005;May, et al., 2005). However, the unique cilia defect of *Arl13b*^{hnn} has unique consequences for Shh signaling. Unlike total-loss-of-cilia mutants, GliR activity is intact in *Arl13b*^{hnn} mutants, because ventral cell fates are dorsally expanded when GliR is removed in *Arl13b*^{hnn} */Gli3* double mutants (Caspary, et al., 2007). At the same time, GliA is not properly modulated in *Arl13b*^{hnn} mutants, since cells that require the highest or lowest levels of Shh are not specified; instead, cells that require intermediate GliA activity (i.e., MNs) are expanded dorsally and ventrally (Caspary, et al., 2007). Thus, the dorsal expansion of Shh signaling in the *Arl13b*^{hnn} neural tube corresponds to an increase in the ratio of GliA/GliR in lateral and dorsal neural cells (Caspary, et al., 2007).

To directly examine the levels of GliA and GliR in the *Arl13b*^{hnn} neural tube, we performed *in situ* hybridization with antisense probes for *Gli1* and *Gli3* on WT and *Arl13b*^{hnn} caudal neural tube sections, since Gli1 can only be an activator and Gli3 is the predominant repressor in the neural tube. Consistent with previous data, we find that *Gli3* is properly expressed in the *Arl13b*^{hnn} dorsal neural tube at levels similar to those observed in WT (Fig. 9E-H). However, the pattern of *Gli1* expression differs between WT and *Arl13b*^{hnn} embryos: in WT embryos, *Gli1* expression is excluded from the dorsal-most cells of the neural tube (Fig. 9A, C), while in *Arl13b*^{hnn} embryos, expression of *Gli1* is shifted dorsally and enriched in the dorsal neural tube (Fig 9B, D). Together with previous findings, these data demonstrate that the balance of GliA/GliR repressor is shifted in the *Arl13b*^{hnn} dorsal neural tube.

The mechanism by which the abnormal Shh signaling environment causes the observed dorsal phenotypes remains unclear, but it is likely related to cross-talk among signaling pathways. The abnormal *Gdf7* expression and aberrant BMP signaling in *Arl13b*^{hnn} mice are reminiscent of the situation in another mouse mutant, where ectopic Gli2 activator prevents expression of the BMP ligands *BMP7* and *Gdf7* (Cho, et al., 2008). Like *Arl13b*^{hnn}, this mutation affects a ciliary protein, Fkbp8, and the mutants have aberrant BMP signaling as measured by loss of *Math1* and *Lhx2* expression and a reduction in Msx1/2 protein levels (Cho, et al., 2008); however, there are important distinctions between the *Arl13b*^{hnn} and *Fkbp8* phenotypes. In *Fkbp8* mutants, the most ventral cell types requiring the highest levels of Gli activator (FP and V3 interneurons) are expanded dorsally. Both the dorsal expansion of ventral cell types and disruption of BMP signaling are abolished in *Fkbp8/Gli2* double mutants, indicating that ectopic Gli2 activator is principally responsible for the *Fkbp8* phenotype (Cho, et al., 2008). In contrast, the phenotype of *Arl13b*^{hnn} mutants is not consistent with an increase in the highest levels of Gli2 activator; instead, the dorsal and ventral expansion of intermediate cell types (MNs) are consistent with constitutive, intermediate-level activation of Gli (Caspary, et al., 2007). Furthermore, removing the major Gli activator in the *Arl13b*^{hnn} mutant background (via *Arl13b*^{hnn}*/Gli2* double mutants) does not rescue all the *Arl13b*^{hnn} patterning defects (Caspary, et al., 2007). Specifically, the dorsal expansion of MNs persists in *Arl13b*^{hnn}*/Gli2* doubles, illustrating that ectopically active Gli2 in the *Arl13b*^{hnn} neural tube is not sufficient to explain the loss of BMP ligand expression. Since *Gli1* was found to be dorsally enriched in *Arl13b*^{hnn} and *Gli1* also promotes the differentiation of MNs (Ruiz i Altaba, 1998), the dorsal expansion of MNs in *Arl13b*^{hnn}*/Gli2* double mutants is likely due to changes in the position and/or activity of Gli1

activator. Thus, one interpretation of these data would posit a new role for Shh signaling in the modulation of the BMP signaling pathway: namely, that ectopic Gli1 activator activity can prevent *Gdf7* expression and disrupt BMP signaling.

Normal Wnt response in the absence of ligand may reveal sensitivity of β-catenin

Most enigmatic is our result showing canonical Wnt signaling occurs normally in the absence of ligand in the *Arl13b*^{hnn} neural tube. Since *Wnt1* and *Wnt3a* are expressed in the rostral neural tube and in portions of the caudal neural tube, one possibility is that Wnt ligands from one area diffuse into regions lacking Wnt ligand in the *Arl13b*^{hnn} caudal neural tube; however, this seems unlikely, given that Wnts are secreted glycoproteins that are bound by the extracellular matrix and diffuse over a distance of just a few cell diameters (Bradley and Brown, 1990;Gonzalez, et al., 1991;van den Heuvel, et al., 1989). Another possibility is that early Wnt signals from the surface ectoderm are normal, allowing the Wnt response to be maintained in the dorsal neural tube over time in the absence of ligand, but conditional loss of β-catenin at E9.5, after the neural tube has formed, results in loss of *Olig3* expression by E12.5 (Zechner, et al., 2007), a time point at which we still see normal Olig3 in *Arl13b*^{hnn} mutants (Fig. 1F, H.) A third possibility is that a downstream signaling component, such as β-catenin, is not properly regulated in *Arl13b*^{hnn} mutants. Misregulation of β-catenin has been shown to occur in cells that lack cilia (Corbit, et al., 2008) or basal body proteins (Gerdes, et al., 2007). While it is well established that cilia are required for non-canonical Wnt signaling (Gerdes, et al., 2007;Jones, et al., 2008;Ross, et al., 2005), the data surrounding cilia and canonical Wnt signaling remain controversial. Several components of the canonical Wnt pathway physically localize to cilia, including β-catenin and a negative regulator of canonical Wnt signaling, the APC complex (Corbit, et al., 2008). Further, the inactive, phosphorylated form of β-catenin localizes to the base of the cilium, suggesting that the cilium directly restrains Wnt signaling (Corbit, et al., 2008). Nonetheless, studies that test this hypothesis using mouse mutants or cells derived from mouse mutants have yielded different results. For instance, cells in culture that either completely lack cilia or have shortened cilia show hyper-responsive activation of the canonical Wnt pathway in response to *Wnt3a* stimulation in one study (Corbit, et al., 2008), but not in others (Ocbina, et al., 2009). If cilia are required to restrain canonical Wnt signaling, our results might be explained simply by the short cilia in *Arl13b*^{hnn} mutants. In this scenario, the short cilia cause active β-catenin to be stabilized in the cytoplasm of *Arl13b*^{hnn} mutant cells, allowing Wnt signaling to occur in the absence of ligand. If this hypothesis is correct, we predict that in *Arl13b*$^{\Delta Pax3\text{-}cre}$ conditionals, which show normal Wnt ligand expression, we will see hyper-responsive canonical Wnt signaling. To test this hypothesis, we examined *Axin2* expression in our conditional mutants. At E11.5, *Axin2* expression is identical in *Arl13b*$^{\Delta Pax3\text{-}cre}$ conditionals and controls, both in whole embryos and neural tube sections (Fig. 10). Even though this result is not consistent with cilia being required to restrain canonical Wnt signaling, there is the possibility of a more indirect relationship, in which the abnormal cilia in *Arl13b*^{hnn} disrupts non-canonical Wnt (PCP) signaling, which in turn stabilizes β-catenin and affects canonical Wnt signaling (Brembeck, et al., 2004;Schwarz-Romond, et al., 2002).

A final possibility to explain how canonical Wnt signaling could occur in the absence of ligand in the *Arl13b*^{hnn} neural tube is that, as with the BMP signaling defects, the abnormal Shh signaling environment is principally responsible. The physical interaction between Gli3 repressor and β-catenin allows us to put forward one speculative model of how Wnt signaling might occur in the absence of both Wnt ligands in the *Arl13b*^{hnn} dorsal neural tube. Normally, there is a delicate balance in the dorsal neural tube between the level of Shh signaling, the amount of Gli3R, and Wnt signaling. Excessive Gli3R inhibits canonical Wnt signaling by binding to the active form of β-catenin (Ulloa, et al., 2007). This situation

occurs in *Shh* null embryos, because most of the available Gli3 is processed to become Gli3R (Ulloa, et al., 2007). This implies that in WT embryos, Shh signaling in the dorsal neural tube regulates the available Gli3R, so there is sufficient free active β-catenin for Wnt signaling. In *Arl13b*^{hnn} mutants, increased GliA activity in the dorsal neural tube might effectively lower the amount of Gli3R. Although not sufficient to abolish Gli3R activity, this may tip the balance enough to free some active β-catenin, permitting Wnt signaling or the maintenance of Wnt response in the absence of ligand.

Supplementary Material

Refer to Web version on PubMed Central for supplementary material.

Acknowledgments

This work was supported by NIH grant R01NS056380 to T.C. and a Ruth L. Kirschstein National Research Service Award 1F32HD060368-01A2 to V.L.H. We thank all the members of the Caspary lab as well as Cheryl Timms Strauss for helpful suggestions on the manuscript, and Carmen Birchmeier for Olig3, Foxd3, and Tlx3 antibodies. The HB9 antibody, developed by T. Jessell (Columbia University, New York, NY), was obtained from the Developmental Studies Hybridoma Bank developed under the auspices of the NICHD and maintained by The University of Iowa, Department of Biology, Iowa City, IA 52242.

References

Alvarez-Medina R, Cayuso J, Okubo T, Takada S, Marti E. Wnt canonical pathway restricts graded Shh/Gli patterning activity through the regulation of Gli3 expression. Development. 2008; 135:237–247. [PubMed: 18057099]

Antoshechkin I, Han M. The C. elegans evl-20 gene is a homolog of the small GTPase ARL2 and regulates cytoskeleton dynamics during cytokinesis and morphogenesis. Dev Cell. 2002; 2:579–591. [PubMed: 12015966]

Arber S, Han B, Mendelsohn M, Smith M, Jessell TM, Sockanathan S. Requirement for the homeobox gene Hb9 in the consolidation of motor neuron identity. Neuron. 1999; 23:659–674. [PubMed: 10482234]

Aza-Blanc P, Lin HY, Ruiz i Altaba A, Kornberg TB. Expression of the vertebrate Gli proteins in Drosophila reveals a distribution of activator and repressor activities. Development. 2000; 127:4293–4301. [PubMed: 10976059]

Belo JA, Bouwmeester T, Leyns L, Kertesz N, Gallo M, Follettie M, De Robertis EM. Cerberus-like is a secreted factor with neutralizing activity expressed in the anterior primitive endoderm of the mouse gastrula. Mech Dev. 1997; 68:45–57. [PubMed: 9431803]

Beppu H, Kawabata M, Hamamoto T, Chytil A, Minowa O, Noda T, Miyazono K. BMP type II receptor is required for gastrulation and early development of mouse embryos. Dev Biol. 2000; 221:249–258. [PubMed: 10772805]

Bermingham NA, Hassan BA, Wang VY, Fernandez M, Banfi S, Bellen HJ, Fritzsch B, Zoghbi HY. Proprioceptor pathway development is dependent on Math1. Neuron. 2001; 30:411–422. [PubMed: 11395003]

Bradley RS, Brown AM. The proto-oncogene int-1 encodes a secreted protein associated with the extracellular matrix. EMBO J. 1990; 9:1569–1575. [PubMed: 2158444]

Brembeck FH, Schwarz-Romond T, Bakkers J, Wilhelm S, Hammerschmidt M, Birchmeier W. Essential role of BCL9-2 in the switch between beta-catenin's adhesive and transcriptional functions. Genes Dev. 2004; 18:2225–2230. [PubMed: 15371335]

Caspary T, Larkins CE, Anderson KV. The graded response to Sonic Hedgehog depends on cilia architecture. Dev Cell. 2007; 12:767–778. [PubMed: 17488627]

Cayuso J, Marti E. Morphogens in motion: growth control of the neural tube. J Neurobiol. 2005; 64:376–387. [PubMed: 16041754]

Cho A, Ko HW, Eggenschwiler JT. FKBP8 cell-autonomously controls neural tube patterning through a Gli2- and Kif3a-dependent mechanism. Dev Biol. 2008; 321:27–39. [PubMed: 18590716]

Corbit KC, Shyer AE, Dowdle WE, Gaulden J, Singla V, Chen MH, Chuang PT, Reiter JF. Kif3a constrains beta-catenin-dependent Wnt signalling through dual ciliary and non-ciliary mechanisms. Nat Cell Biol. 2008; 10:70–76. [PubMed: 18084282]

Dickinson ME, Krumlauf R, McMahon AP. Evidence for a mitogenic effect of Wnt-1 in the developing mammalian central nervous system. Development. 1994; 120:1453–1471. [PubMed: 8050356]

Dudley AT, Lyons KM, Robertson EJ. A requirement for bone morphogenetic protein-7 during development of the mammalian kidney and eye. Genes Dev. 1995; 9:2795–2807. [PubMed: 7590254]

Dudley AT, Robertson EJ. Overlapping expression domains of bone morphogenetic protein family members potentially account for limited tissue defects in BMP7 deficient embryos. Dev Dyn. 1997; 208:349–362. [PubMed: 9056639]

Engleka KA, Gitler AD, Zhang M, Zhou DD, High FA, Epstein JA. Insertion of Cre into the Pax3 locus creates a new allele of Splotch and identifies unexpected Pax3 derivatives. Dev Biol. 2005; 280:396–406. [PubMed: 15882581]

Furuta Y, Piston DW, Hogan BL. Bone morphogenetic proteins (BMPs) as regulators of dorsal forebrain development. Development. 1997; 124:2203–2212. [PubMed: 9187146]

Garcia-Garcia MJ, Eggenschwiler JT, Caspary T, Alcorn HL, Wyler MR, Huangfu D, Rakeman AS, Lee JD, Feinberg EH, Timmer JR, Anderson KV. Analysis of mouse embryonic patterning and morphogenesis by forward genetics. Proc Natl Acad Sci U S A. 2005; 102:5913–5919. [PubMed: 15755804]

Gerdes JM, Liu Y, Zaghloul NA, Leitch CC, Lawson SS, Kato M, Beachy PA, Beales PL, DeMartino GN, Fisher S, Badano JL, Katsanis N. Disruption of the basal body compromises proteasomal function and perturbs intracellular Wnt response. Nat Genet. 2007; 39:1350–1360. [PubMed: 17906624]

Gonzalez F, Swales L, Bejsovec A, Skaer H, Martinez Arias A. Secretion and movement of wingless protein in the epidermis of the Drosophila embryo. Mech Dev. 1991; 35:43–54. [PubMed: 1720017]

Gowan K, Helms AW, Hunsaker TL, Collisson T, Ebert PJ, Odom R, Johnson JE. Crossinhibitory activities of Ngn1 and Math1 allow specification of distinct dorsal interneurons. Neuron. 2001; 31:219–232. [PubMed: 11502254]

Helms AW, Johnson JE. Specification of dorsal spinal cord interneurons. Curr Opin Neurobiol. 2003; 13:42–49. [PubMed: 12593981]

Hoyt MA, Stearns T, Botstein D. Chromosome instability mutants of Saccharomyces cerevisiae that are defective in microtubule-mediated processes. Mol Cell Biol. 1990; 10:223–234. [PubMed: 2403635]

Huangfu D, Anderson KV. Cilia and Hedgehog responsiveness in the mouse. Proc Natl Acad Sci U S A. 2005; 102:11325–11330. [PubMed: 16061793]

Huangfu D, Liu A, Rakeman AS, Murcia NS, Niswander L, Anderson KV. Hedgehog signalling in the mouse requires intraflagellar transport proteins. Nature. 2003; 426:83–87. [PubMed: 14603322]

Ingham PW, McMahon AP. Hedgehog signaling in animal development: paradigms and principles. Genes Dev. 2001; 15:3059–3087. [PubMed: 11731473]

Jacob J, Briscoe J. Gli proteins and the control of spinal-cord patterning. EMBO Rep. 2003; 4:761–765. [PubMed: 12897799]

Jessell TM. Neuronal specification in the spinal cord: inductive signals and transcriptional codes. Nat Rev Genet. 2000; 1:20–29. [PubMed: 11262869]

Jho EH, Zhang T, Domon C, Joo CK, Freund JN, Costantini F. Wnt/beta-catenin/Tcf signaling induces the transcription of Axin2, a negative regulator of the signaling pathway. Mol Cell Biol. 2002; 22:1172–1183. [PubMed: 11809808]

Jones C, Roper VC, Foucher I, Qian D, Banizs B, Petit C, Yoder BK, Chen P. Ciliary proteins link basal body polarization to planar cell polarity regulation. Nat Genet. 2008; 40:69–77. [PubMed: 18066062]

Kahn RA, Cherfils J, Elias M, Lovering RC, Munro S, Schurmann A. Nomenclature for the human Arf family of GTP-binding proteins: ARF, ARL, and SAR proteins. J Cell Biol. 2006; 172:645–650. [PubMed: 16505163]

Lee KJ, Dietrich P, Jessell TM. Genetic ablation reveals that the roof plate is essential for dorsal interneuron specification. Nature. 2000; 403:734–740. [PubMed: 10693795]

Lee KJ, Mendelsohn M, Jessell TM. Neuronal patterning by BMPs: a requirement for GDF7 in the generation of a discrete class of commissural interneurons in the mouse spinal cord. Genes Dev. 1998; 12:3394–3407. [PubMed: 9808626]

Li Y, Kelly WG, Logsdon JM Jr, Schurko AM, Harfe BD, Hill-Harfe KL, Kahn RA. Functional genomic analysis of the ADP-ribosylation factor family of GTPases: phylogeny among diverse eukaryotes and function in C. elegans. Faseb J. 2004; 18:1834–1850. [PubMed: 15576487]

Liem KF Jr, Tremml G, Jessell TM. A role for the roof plate and its resident TGFbeta-related proteins in neuronal patterning in the dorsal spinal cord. Cell. 1997; 91:127–138. [PubMed: 9335341]

Liu A, Niswander LA. Bone morphogenetic protein signalling and vertebrate nervous system development. Nat Rev Neurosci. 2005; 6:945–954. [PubMed: 16340955]

Liu A, Wang B, Niswander LA. Mouse intraflagellar transport proteins regulate both the activator and repressor functions of Gli transcription factors. Development. 2005; 132:3103–3111. [PubMed: 15930098]

Liu F, Massague J, Ruiz i Altaba A. Carboxy-terminally truncated Gli3 proteins associate with Smads. Nat Genet. 1998; 20:325–326. [PubMed: 9843199]

Liu Y, Helms AW, Johnson JE. Distinct activities of Msx1 and Msx3 in dorsal neural tube development. Development. 2004; 131:1017–1028. [PubMed: 14973289]

Luo G, Hofmann C, Bronckers AL, Sohocki M, Bradley A, Karsenty G. BMP-7 is an inducer of nephrogenesis, and is also required for eye development and skeletal patterning. Genes Dev. 1995; 9:2808–2820. [PubMed: 7590255]

Lyons KM, Hogan BL, Robertson EJ. Colocalization of BMP 7 and BMP 2 RNAs suggests that these factors cooperatively mediate tissue interactions during murine development. Mech Dev. 1995; 50:71–83. [PubMed: 7605753]

Maretto S, Cordenonsi M, Dupont S, Braghetta P, Broccoli V, Hassan AB, Volpin D, Bressan GM, Piccolo S. Mapping Wnt/beta-catenin signaling during mouse development and in colorectal tumors. Proc Natl Acad Sci U S A. 2003; 100:3299–3304. [PubMed: 12626757]

Matise MP, Joyner AL. Gli genes in development and cancer. Oncogene. 1999; 18:7852–7859. [PubMed: 10630638]

May SR, Ashique AM, Karlen M, Wang B, Shen Y, Zarbalis K, Reiter J, Ericson J, Peterson AS. Loss of the retrograde motor for IFT disrupts localization of Smo to cilia and prevents the expression of both activator and repressor functions of Gli. Dev Biol. 2005; 287:378–389. [PubMed: 16229832]

McMahon JA, Takada S, Zimmerman LB, Fan CM, Harland RM, McMahon AP. Noggin-mediated antagonism of BMP signaling is required for growth and patterning of the neural tube and somite. Genes Dev. 1998; 12:1438–1452. [PubMed: 9585504]

Megason SG, McMahon AP. A mitogen gradient of dorsal midline Wnts organizes growth in the CNS. Development. 2002; 129:2087–2098. [PubMed: 11959819]

Mishina Y, Suzuki A, Ueno N, Behringer RR. Bmpr encodes a type I bone morphogenetic protein receptor that is essential for gastrulation during mouse embryogenesis. Genes Dev. 1995; 9:3027–3037. [PubMed: 8543149]

Muller T, Anlag K, Wildner H, Britsch S, Treier M, Birchmeier C. The bHLH factor Olig3 coordinates the specification of dorsal neurons in the spinal cord. Genes Dev. 2005; 19:733–743. [PubMed: 15769945]

Muroyama Y, Fujihara M, Ikeya M, Kondoh H, Takada S. Wnt signaling plays an essential role in neuronal specification of the dorsal spinal cord. Genes Dev. 2002; 16:548–553. [PubMed: 11877374]

Nagy, A.; Gertsenstein, M.; Vintersten, K.; Behringer, R. Manipulating the Mouse Embryo: A Laboratory Manual. 3. Cold Spring Harbor Laboratory Press; Cold Spring Harbor, New York: 2003.

Novitch BG, Chen AI, Jessell TM. Coordinate regulation of motor neuron subtype identity and pan-neuronal properties by the bHLH repressor Olig2. Neuron. 2001; 31:773–789. [PubMed: 11567616]

Ocbina PJ, Tuson M, Anderson KV. Primary cilia are not required for normal canonical Wnt signaling in the mouse embryo. PLoS One. 2009; 4:e6839. [PubMed: 19718259]

Parr BA, Shea MJ, Vassileva G, McMahon AP. Mouse Wnt genes exhibit discrete domains of expression in the early embryonic CNS and limb buds. Development. 1993; 119:247–261. [PubMed: 8275860]

Qian Y, Shirasawa S, Chen CL, Cheng L, Ma Q. Proper development of relay somatic sensory neurons and D2/D4 interneurons requires homeobox genes Rnx/Tlx-3 and Tlx-1. Genes Dev. 2002; 16:1220–1233. [PubMed: 12023301]

Radcliffe PA, Vardy L, Toda T. A conserved small GTP-binding protein Alp41 is essential for the cofactor-dependent biogenesis of microtubules in fission yeast. FEBS Lett. 2000; 468:84–88. [PubMed: 10683446]

Ribes V, Briscoe J. Establishing and interpreting graded Sonic Hedgehog signaling during vertebrate neural tube patterning: the role of negative feedback. Cold Spring Harb Perspect Biol. 2009; 1:a002014. [PubMed: 20066087]

Ross AJ, May-Simera H, Eichers ER, Kai M, Hill J, Jagger DJ, Leitch CC, Chapple JP, Munro PM, Fisher S, Tan PL, Phillips HM, Leroux MR, Henderson DJ, Murdoch JN, Copp AJ, Eliot MM, Lupski JR, Kemp DT, Dollfus H, Tada M, Katsanis N, Forge A, Beales PL. Disruption of Bardet-Biedl syndrome ciliary proteins perturbs planar cell polarity in vertebrates. Nat Genet. 2005; 37:1135–1140. [PubMed: 16170314]

Ruiz i Altaba A. Combinatorial Gli gene function in floor plate and neuronal inductions by Sonic hedgehog. Development. 1998; 125:2203–2212. [PubMed: 9584120]

Schaeren-Wiemers N, Gerfin-Moser A. A single protocol to detect transcripts of various types and expression levels in neural tissue and cultured cells: in situ hybridization using digoxigenin-labelled cRNA probes. Histochemistry. 1993; 100:431–440. [PubMed: 7512949]

Schneider L, Clement CA, Teilmann SC, Pazour GJ, Hoffmann EK, Satir P, Christensen ST. PDGFRalphaalpha signaling is regulated through the primary cilium in fibroblasts. Curr Biol. 2005; 15:1861–1866. [PubMed: 16243034]

Schwarz-Romond T, Asbrand C, Bakkers J, Kuhl M, Schaeffer HJ, Huelsken J, Behrens J, Hammerschmidt M, Birchmeier W. The ankyrin repeat protein Diversin recruits Casein kinase Iepsilon to the beta-catenin degradation complex and acts in both canonical Wnt and Wnt/JNK signaling. Genes Dev. 2002; 16:2073–2084. [PubMed: 12183362]

Solloway MJ, Robertson EJ. Early embryonic lethality in Bmp5;Bmp7 double mutant mice suggests functional redundancy within the 60A subgroup. Development. 1999; 126:1753–1768. [PubMed: 10079236]

Soriano P. Generalized lacZ expression with the ROSA26 Cre reporter strain. Nat Genet. 1999; 21:70–71. [PubMed: 9916792]

Su CY, Hillman MJ, Caspary T. Sonic hedgehog acts first as an instructive morphogen and then as a permissive signal in mammalian neural tube patterning. unpublished data.

Su CY, Peyrot SM, Hillman MJ, Harland RM, Wallingford JB, Caspary T. Conserved developmental constraints on Shh as a morphogen in the neural tube. in preparation.

Ulloa F, Itasaki N, Briscoe J. Inhibitory Gli3 activity negatively regulates Wnt/beta-catenin signaling. Curr Biol. 2007; 17:545–550. [PubMed: 17331723]

van den Heuvel M, Nusse R, Johnston P, Lawrence PA. Distribution of the wingless gene product in Drosophila embryos: a protein involved in cell-cell communication. Cell. 1989; 59:739–749. [PubMed: 2582493]

Veland IR, Awan A, Pedersen LB, Yoder BK, Christensen ST. Primary cilia and signaling pathways in mammalian development, health and disease. Nephron Physiol. 2009; 111:p39–53. [PubMed: 19276629]

Wine-Lee L, Ahn KJ, Richardson RD, Mishina Y, Lyons KM, Crenshaw EB 3rd. Signaling through BMP type 1 receptors is required for development of interneuron cell types in the dorsal spinal cord. Development. 2004; 131:5393–5403. [PubMed: 15469980]

Winnier G, Blessing M, Labosky PA, Hogan BL. Bone morphogenetic protein-4 is required for mesoderm formation and patterning in the mouse. Genes Dev. 1995; 9:2105–2116. [PubMed: 7657163]

Yamada T, Pfaff SL, Edlund T, Jessell TM. Control of cell pattern in the neural tube: motor neuron induction by diffusible factors from notochord and floor plate. Cell. 1993; 73:673–686. [PubMed: 8500163]

Yu W, McDonnell K, Taketo MM, Bai CB. Wnt signaling determines ventral spinal cord cell fates in a time-dependent manner. Development. 2008; 135:3687–3696. [PubMed: 18927156]

Zechner D, Muller T, Wende H, Walther I, Taketo MM, Crenshaw EB 3rd, Treier M, Birchmeier W, Birchmeier C. Bmp and Wnt/beta-catenin signals control expression of the transcription factor Olig3 and the specification of spinal cord neurons. Dev Biol. 2007; 303:181–190. [PubMed: 17150208]

Zhang H, Bradley A. Mice deficient for BMP2 are nonviable and have defects in amnion/chorion and cardiac development. Development. 1996; 122:2977–2986. [PubMed: 8898212]

Zhou C, Cunningham L, Marcus AI, Li Y, Kahn RA. Arl2 and Arl3 regulate different microtubule-dependent processes. Mol Biol Cell. 2006; 17:2476–2487. [PubMed: 16525022]

Research highlights

- *Arl13b*^{hnn} dorsal patterning defects result from abnormal BMP signaling
- Wnt ligand expression is abnormal, but downstream Wnt signaling is normal in *Arl13b*^{hnn} mutants
- Arl13b is required non-autonomously for BMP signaling and Wnt ligand expression
- Anomalies in the Gli activator/Gli repressor ratio may account for the *Arl13b*^{hnn} dorsal patterning defects

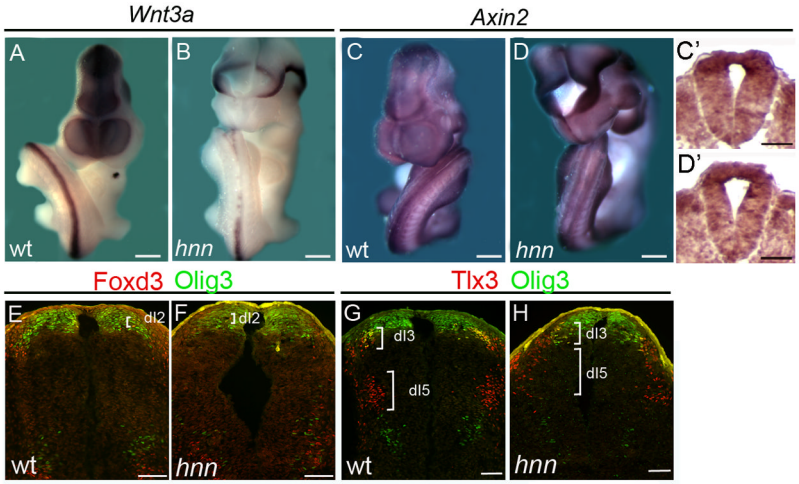

Figure 1. Normal Wnt response in the absence of Wnt ligands in *Arl13b*^{hnn} embryos

(A-D) Expression of *Wnt3a* (A and B) and *Axin2* (C and D) in whole E10.5 WT and *Arl13b*^{hnn} embryos. The *Arl13b*^{hnn} embryos pictured here all exhibit mild to moderate spina bifida in the caudal neural tube. Only *Wnt3a* is abnormally expressed in *Arl13b*^{hnn} embryos; it is absent from most of the *Arl13b*^{hnn} caudal neural tube. This was previously shown for the other Wnt ligand in the RP, *Wnt1* (Caspary, et al., 2007). Scale bars in A-D represent approximately 300 microns.

(C', D') Caudal neural tube sections showing *Axin2* expression in the dorsal neural tube of E10.5 WT and *Arl13b*^{hnn} embryos, respectively. Scale bars represent approximately 50 microns.

(E-H) Comparison of the distribution of Olig3 (green) and neuronal subtypes dI2 (marked by Foxd3, red) and dI3/dI5 (marked by Tlx3, red) in E12.5 WT and *Arl13b*^{hnn} caudal neural tube sections. Olig3 is similarly distributed in the caudal neural tube of E12.5 WT and *Arl13b*^{hnn} embryos. Foxd3^{+} (dI2) and Tlx3^{+} (dI3/dI5) cells are observed in *Arl13b*^{hnn}, although the pattern is different from WT. Scale bars represent approximately 50 microns.

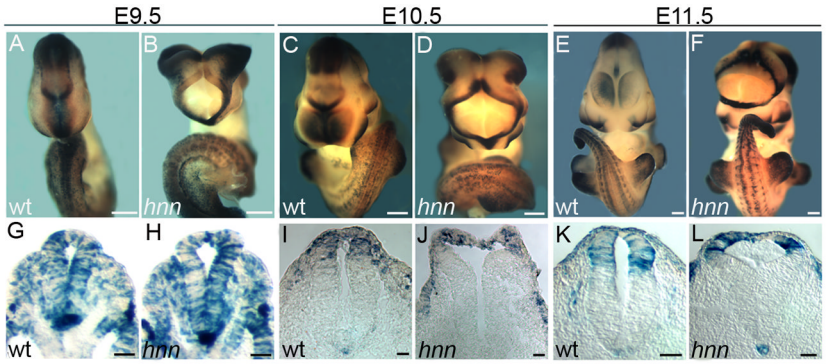

Figure 2. The BATgal reporter shows equivalent canonical Wnt signaling in WT and *Arl13b*^{hnn} embryos

(A-F) Ventral view of E9.5 (A and B), E10.5 (C and D), and E11.5 (E and F) WT and *Arl13b*^{hnn} embryos carrying the BATgal transgene and stained for lacZ activity.

(G-L) Corresponding neural tube sections of the above embryos at the hindlimb level. Scale bars in A-F represent approximately 300 microns. Scale bars in G-L represent approximately 50 microns.

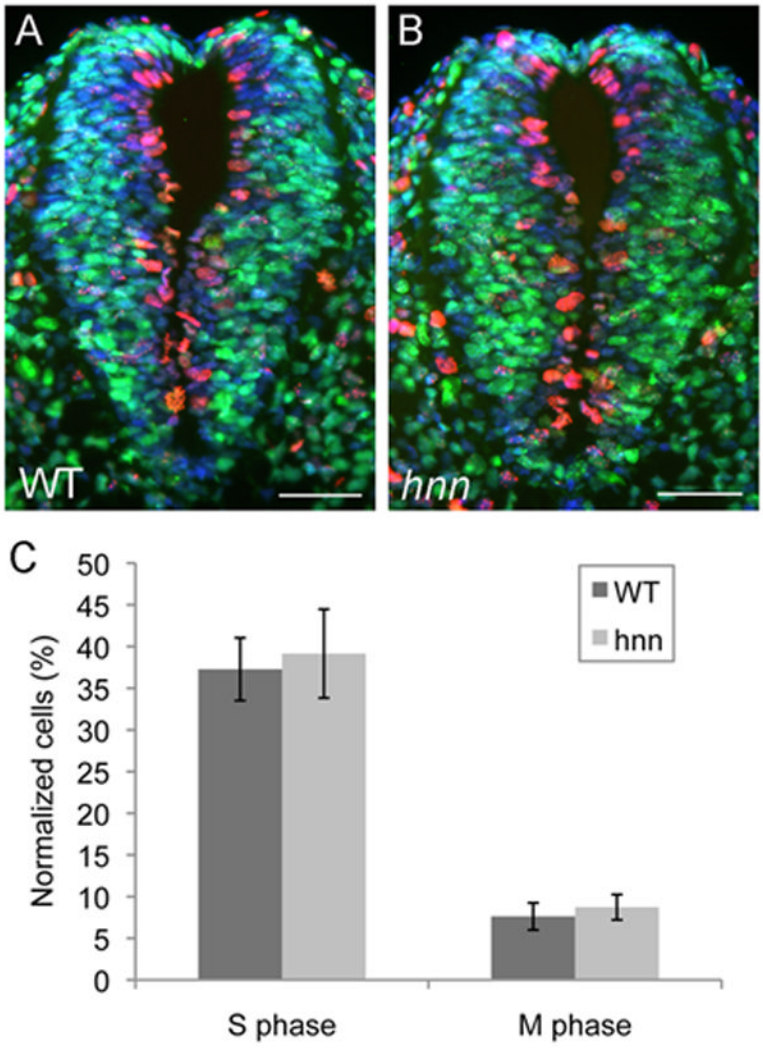

Figure 3. Equivalent cell proliferation in the neural tube of WT and *Arl13b*^{hnn} embryos

(A-B) E10.5 WT (A) and *Arl13b*^{hnn} (B) neural tube sections stained with antibodies against phospho-histone H3 (in red) and BrdU (in green). All cells in the neural tube are stained with Hoechst (blue). Scale bars represent approximately 50 microns.

(C-D) Quantification of the number of cells staining with phospho-histone H3 (in M phase) and the number of cells staining with BrdU (in S phase). Cells were counted in 12 neural tube sections from 3 WT embryos and 15 neural tube sections from 3 *Arl13b*^{hnn} embryos. To account for neural tube size differences, the number of cells in S phase and M phase were normalized to the total number of cells in the neural tube and expressed as a percentage.

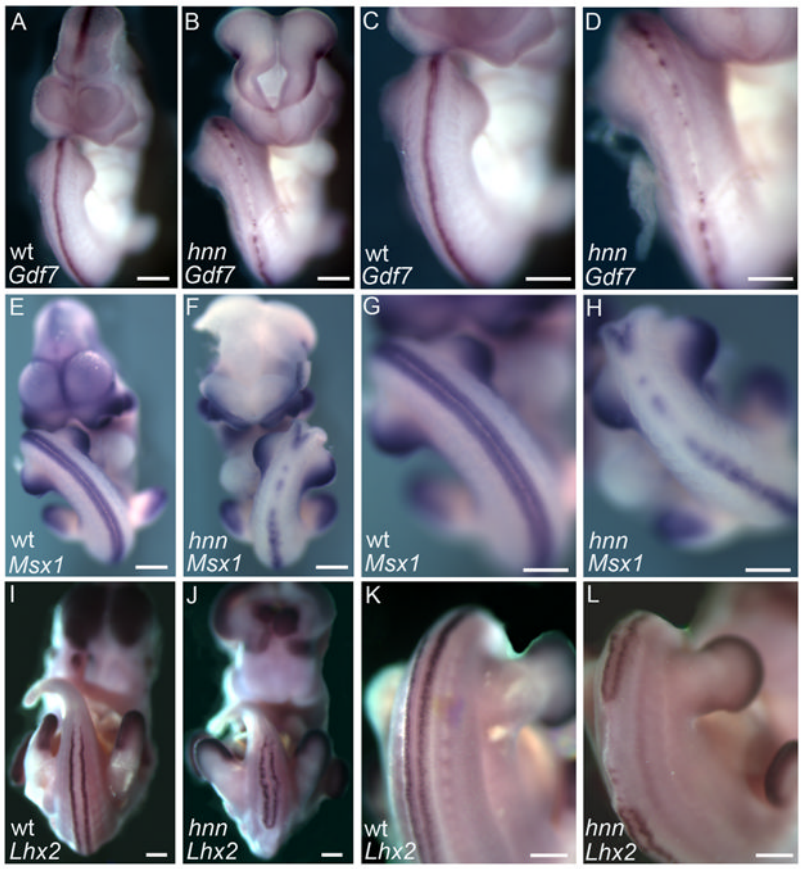

Figure 4. BMP signaling is disrupted in *Arl13b*^{hnn} embryos

(A-D) Expression of the BMP ligand *Gdf7* is discontinuous/absent in the caudal neural tube of E10.5 *Arl13b*^{hnn} embryos. C and D are higher-magnification views of the region of interest.

(E-L) Expression of the BMP pathway target genes *Msx1* (E-H) and *Lhx2* (I-L) is discontinuous/absent in the caudal neural tube of E10.5 and E12.5 *Arl13b*^{hnn} embryos, respectively. G, H, K, and L are higher-magnification views of the region of interest. Scale bars represent approximately 300 microns.

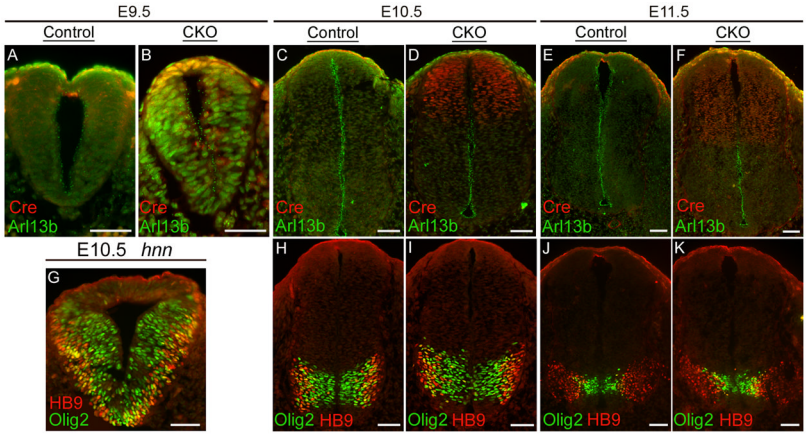

Figure 5. In *Arl13b*$^{\Delta Pax3\text{-}cre}$ embryos, Arl13b is deleted in the dorsal neural tube, and ventral patterning is normal

(A-F) Caudal neural tube sections of E9.5 (A and B), E10.5 (C and D), and E11.5 (E and F) control and *Arl13b*$^{\Delta Pax3\text{-}cre}$ (CKO) embryos stained with anti-Arl13b (green) and anti-Cre (red). Arl13b is particularly apparent in cells that line the ventricular zone. Control embryos lack Cre recombinase.

(G-K) Caudal neural tube sections of E10.5 *Arl13b*^{hnn} (G), E10.5 control and *Arl13b*$^{\Delta}$*Pax3-*^{cre} (H and I), and E11.5 control and *Arl13b*$^{\Delta Pax3\text{-}cre}$ (J and K) embryos stained with anti-Olig2 (green) and anti-HB9 (red). Olig2 marks motor neuron progenitors, and HB9 marks motor neurons. Scale bars represent approximately 50 microns.

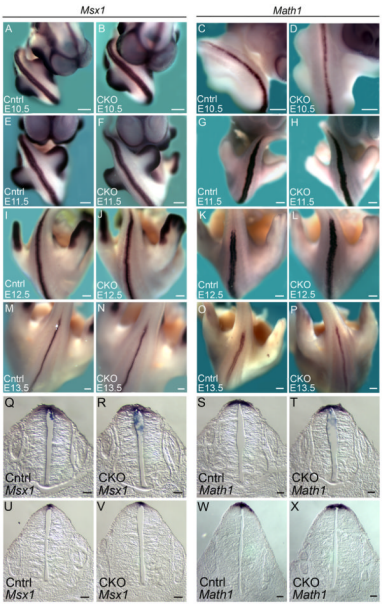

Figure 6. *Msx1* and *Math1* are expressed normally in *Arl13b*$^{\Delta Pax3\text{-}cre}$ embryos

(A-P) Expression of *Msx1* (A, B, E, F, I, J, M and N) and *Math1* (C, D, G, H, K, L, O and P) in whole control (Cntrl) and *Arl13b*$^{\Delta Pax3\text{-}cre}$ (CKO) embryos at E10.5 (A-D), E11.5 (EH), E12.5 (I-L), and E13.5 (M-P). Scale bars represent approximately 300 microns. (Q-X) Neural tube sections of the above embryos, taken at the hindlimb level of E11.5 (Q-T) and E12.5 (U-X) control and *Arl13b*$^{\Delta Pax3\text{-}cre}$ (CKO) embryos. Scale bars represent approximately 50 microns.

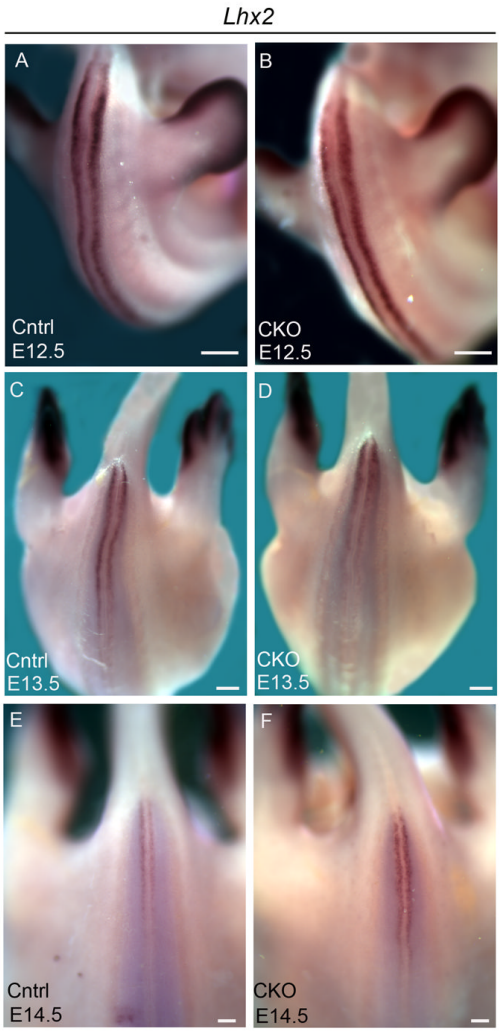

Figure 7. *Lhx2* is expressed normally in *Arl13b*$^{\Delta Pax3\text{-}cre}$ embryos

(A-F) Expression of *Lhx2* in whole control (Cntrl) and *Arl13b*$^{\Delta Pax3\text{-}cre}$ (CKO) embryos at E12.5 (A and B), E13.5 (C and D), and E14.5 (E and F). Scale bars represent approximately 300 microns.

Figure 8. Both the BMP and Wnt ligands and the dorsal marker *Mash1* are expressed normally in *Arl13b*$^{\Delta Pax3\text{-}cre}$ embryos

(A-D) *Gdf7* expression in E11.5 (A and B) and E12.5 (C and D) control (Cntrl) and *Arl13b*$^{\Delta Pax3\text{-}cre}$ (CKO) embryos.

(E-L) *Wnt1* (E-H) and *Wnt3a* (I-L) expression in E11.5 (E, F, I, J) and E12.5 (G, H, K, L) control (Cntrl) and *Arl13b*$^{\Delta Pax3\text{-}cre}$ (CKO) embryos.

(M-N) *Mash1* expression in E11.5 (M and N) and E12.5 (O and P) control (Cntrl) and *Arl13b*$^{\Delta Pax3\text{-}cre}$ (CKO) embryos. Scale bars represent approximately 300 microns.

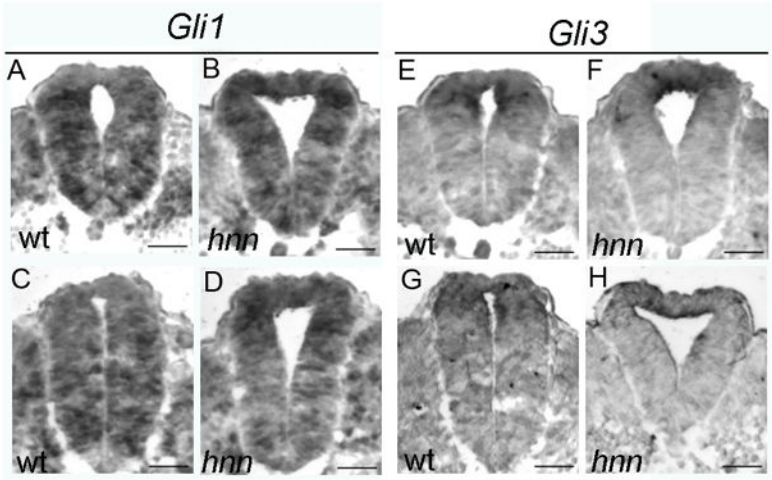

Figure 9. The ratio of GliA/GliR is disrupted in *Arl13b*^{hnn} embryos

(A-D) *Gli1* expression in E10.5 WT (A, C) and *Arl13b*^{hnn} (B, D) caudal neural tube sections. Sections C and D are slightly more rostral than A and B. (E-H) *Gli3* expression in E10.5 WT (E, G) and *Arl13b*^{hnn} (F, H) caudal neural tube sections. Sections G and H are slightly more rostral than E and F. Scale bars represent approximately 50 microns.

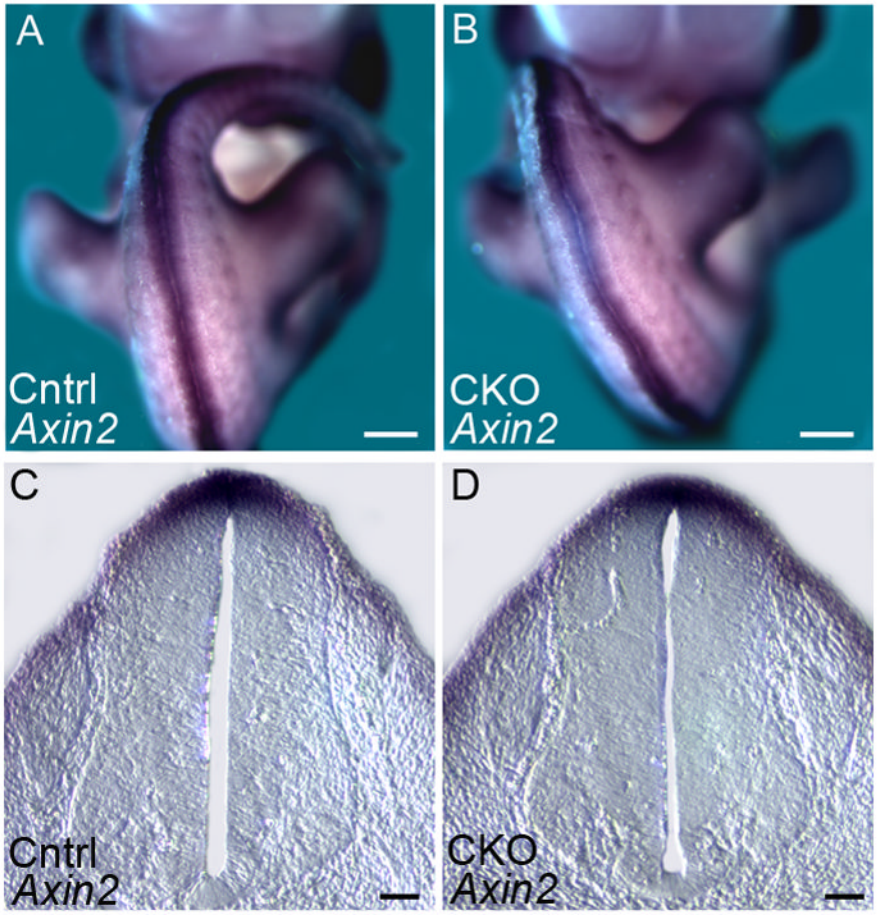

Figure 10. ***Axin2*** **is not overexpressed in** ***Arl13b*** $^{\Delta Pax3\text{-}cre}$ **embryos**

(A and B) *Axin2* is expressed at identical levels in E11.5 control (Cntrl) and *Arl13b*$^{\Delta}$*Pax3-*^{cre} (CKO) embryos. Scale bars represent approximately 300 microns.

(C and D) Neural tube sections taken at the hindlimb level of the above control (Cntrl) and *Arl13b*$^{\Delta Pax3\text{-}cre}$ (CKO) embryos. Scale bars represent approximately 50 microns.

Table 1

Survival of *Arl13b*$^{\Delta Pax3\text{-}cre}$ mutants at various time points before and after birth. *Arl13b*$^{\Delta Pax3\text{-}cre}$ mutants are able to survive *in utero* up until birth; however, immediately after birth 90% die from an apparent breathing problem.

	E14.5 (all alive)	E17.5 (all alive)	E19.5 (all alive)	P0		P21	
				Alive	Dead	Alive	Dead
Arl13b$^{\Delta Pax3\text{-}cre}$	3	2	2		9		1
Control	5	4	5	25	3	25	0
Total	8	6	7	26	12	25	1